Microwave Heating Cavities: Modelling and Analysis

Bratislav Milovanović, Nebojša Dončov, Jugoslav Joković

Abstract – **In this paper, cylindrical metallic cavities used in the processes of dielectric materials heating and drying by microwave energy, are discussed. Their mode tuning behaviour under different loading and excitation conditions has been presented. A short review of techniques used for modelling and analysis purposes as well as the numerical results mostly experimentally verified are given.**

Keywords – **microwave cavity, load, transverse resonance method, neural networks, TLM method, resonant frequency.**

I. Introduction

Microwave energy for heating and drying dielectric materials finds many uses in domestic, industrial and medical environments. As a result, a numerous microwave applicators have been developed over the years. They come in various shapes and sizes based on the properties, geometry and volume of dielectric materials. Among them, the most popular ones are resonant applicators classified as either single or multimode cylindrical metallic cavities, partially loaded with dielectric materials [1]. The knowledge of the mode tuning behaviour in a cavity under loading condition (i.e. physical and electrical parameters of the load) forms an integral part of the studies in microwave heating and can significantly help in designing these applicators. Thus, the loaded cylindrical metallic cavities have been the research subject of a number of authors.

In general, the published results have been addressed mostly to the cylindrical cavity with rectangular cross-section [2-8] loaded with multilayer plan parallel dielectric slabs. This is a simple configuration suitable for good modelling of some practical heating and drying equipment. A cylindrical cavity with circular cross-section has been considered too [9-12], as a structure widely used in the processes of permittivity and loss measuring of dielectric materials. Theoretical analysis was based on the application of transverse resonance method (TRM) [13], a classical approach for this type of problems. This simple method allows for resonant frequencies calculation from the characteristic equation which is transcendental for lossless homogeneous [5,6], complex transcendental for lossy homogeneous [10] and integral for lossy inhomogeneous dielectric slab [7]. In order to solve the characteristic equation, an appropriate numerical technique with an efficient procedure for mode identification [8] was required. Also, some of the results of theoretical investigation were accompanying with the experimental work and the comparisons between measured and computed resonant frequencies were reported in references [9,11]. The main shortage of TRM is incapability of considering dielectric slabs with different shape than plan parallel.

A numerical simple approximate procedure which does not require a use of complex mathematical technique is suggested in [14]. Using this approach the resonant frequencies in the cylindrical metallic cavities loaded by lossless and low loss dielectric slabs could be determined approximately from the network of resonant and anti-resonant curves obtained separately in air and dielectric part of the cavity. At the moment, the application of this procedure is limited to the case of one dielectric slab placed at the bottom of the cavity.

Neural networks represent good alternative to classical approach in microwave heating area, allowing for faster and more accurate calculation of resonant frequencies. In reference [15], a classical multilayer perception (MLP) network is applied very successfully for modelling of cylindrical microwave cavity applicators. A good characteristic of this network is that belongs to the block box networks i.e. all functional dependences are modelled exclusively on the basic of the training data. However, the requirement of providing the relatively large training set from the TRM is the main disadvantage and it can be overcome with the use of so-called hybrid empirical-neural (HEN) model [16,18]. It is based on choosing an appropriate non-uniform training sample distribution and the neural model training on the basic the resonant frequency differences between results obtained by TRM and approximate approach. Knowledge based neural (KBN) networks [17,18] represent another alternative to MLP approach. The KBNN model integrates the knowledge about the behaviour of the resonant frequencies defined in approximate approach, which results in significantly smaller training set with the same or even higher accuracy than MLP network. However, it is clear that suggested models face up to the same limitations as MTR and approximate approach used for the training of neural networks.

As soon as complicated shapes or structures containing lossy dielectric loads are encountered, previously mentioned techniques are less suitable. As microwave heating applicators fall into one or both of the later categories, computational electromagnetic techniques emerge as an invaluable tool in the cavity design. They particularly allow users to see what is happening inside the cavities, thus empowering them to make necessary changes in order to optimize the cavity design. Numerical modelling provides valuable information on such parameters as the electric and magnetic field and the power absorbed by the load. Several numerical techniques are available for microwave heating studies; among them the

Bratislav Milovanović, Nebojša Dončov and Jugoslav Joković are with the Faculty of Electronic Engineering, Aleksandra Medvedeva 14, 18000 Nis, Serbia and Montenegro, E-mail: [bata, doncov, jugoslav]@elfak.ni.ac.yu

finite difference time domain (FD-TD) [19] and transmission line matrix (TLM) [20], as known as full-wave methods, are most popular in this field [21-25].

The TLM method is a general electromagnetically based numerical method highly suitable for modelling of the structures of complicated geometry. It has been developed and used very successfully to tackle the problems in the area of loaded cylindrical metallic cavities modelling [26-28]. Analysis of flowing type microwave applicators, i.e. tunnel type applicators is presented in [26]. Sufficiently fine non-uniform TLM mesh is applied to model inhomogeneous lossy dielectric load, arbitrary raised above the cavity floor and whose electric parameters vary along its length under temperature influence. Another type of dielectric inhomogeneity as a result of load shape is considered in [27]. Appropriate TLM models are developed in orthogonal curvilinear mesh to describe several regular but complex geometric shapes of the lossy dielectric sample. An influence of real excitation to the resonant frequencies in cylindrical metallic cavity is investigated too, [28]. The straight wire conductor, as a real feed form, is introduced through wire node [29], in order to make TLM model closer to the experimental procedure where a small probe inside the cavity is used as an excitation.

This paper contains a review of previously mentioned techniques, used by members of Laboratory for Microwave Technique and Satellite Television, Faculty of Electronic Engineering, University of Nis, for modelling and analysis purposes of microwave heating cavities. Some characteristic examples of loaded cylindrical metallic cavities will be presented together with the obtained results mostly experimentally verified at the same Laboratory.

II. NUMERICAL TECHNIQUES

A. Approximate procedure

A new approach for approximate determination of resonant frequencies for the case of lossless and low loss dielectric slab placed at the bottom of cylindrical metallic cavities with rectangular, circular and elliptical cross-section [14] will be presented in this section. It is derived from very intensive investigation of mode tuning behaviour in cylindrical metallic cavities loaded with multilayer plan parallel dielectric slabs, conducted over the years. Compared with TRM, it significantly simplifies the resonant frequency calculation and speed up the identification of resonant modes during experimental measurements.

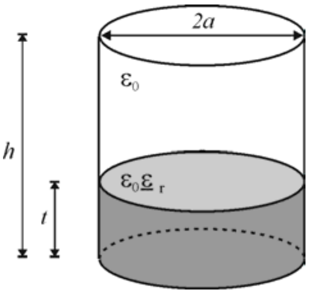

Fig.1 *A circular metallic cavity*

The approximate procedure will be illustrated for the example of circular metallic cavity, radius a and height h, loaded with lossless dielectric slab, thickness t, placed at the bottom of the cavity (Fig.1). For short-circuit boundary (electric wall) at the interface air-dielectric ($z=t$), resonance conditions in air and dielectric part of the cavity are:

$$h - t = \ell \lambda_{t0} / 2 \quad \text{for} \quad \ell = 0,1,2,... \tag{1}$$

$$t = k \frac{\lambda_t}{2} \quad \text{for } k=1,2,\ldots \tag{2}$$

where: λ_{t0} and λ_t are wavelengths of waveguide section, with the same cross-section as cavity, filled with air and dielectric, respectively. Integer number ℓ and k represent the number of *half waves o*f standing wave for electric field in corresponding part of the cavity.

Using the expressions for propagation coefficient in a waveguide filled with air and dielectric [13] and Eqs.(1-2), resonant frequencies versus filling factor t/h in air and dielectric part of the cavity can be found as:

$$f_{ea}^2(t/h) = \left(\ell \frac{f_0}{1-(t/h)} \right)^2 + f_{c0}^2 \quad \text{for} \quad \ell = \begin{cases} 0,1,2,... \ \mathrm{TM}_{\mathrm{mnp}} \\ 1,2,3,... \ \mathrm{TE}_{\mathrm{mnp}} \end{cases} \tag{3}$$

$$f_{ed}^2(t/h) = \left(k \frac{f_0}{\sqrt{\varepsilon_r'}} \frac{1}{t/h} \right)^2 + \left(\frac{f_{c0}}{\sqrt{\varepsilon_r'}} \right)^2 \quad \text{for } k=1,2,\ldots \tag{4}$$

where: $f_{c0} = ck_c/(2\pi)$ and $f_0 = c/(2h)$. Constant k_c is governed by the dimensions of cavity cross-section.

The anti-resonant frequencies versus filling factor t/h in air and dielectric part of cavity given as:

$$f_{ma}^2(t/h) = \left(\frac{2\ell - 1}{2} \frac{f_0}{1-(t/h)} \right)^2 + f_{c0}^2 \quad \text{for} \quad \ell = 1,2,... \tag{5}$$

$$f_{md}^2(t/h) = \left(\frac{2k-1}{2} \frac{f_0}{\sqrt{\varepsilon_r'}} \frac{1}{t/h} \right)^2 + \left(\frac{f_{c0}}{\sqrt{\varepsilon_r'}} \right)^2 \quad \text{for } k=1,2,\ldots \tag{6}$$

can be easily derived applying the open-circuit boundary (magnetic wall) at the plane $z=t$. Resonant and anti-resonant curves versus filling factor, given by Eqs.(3-6), are monotonous increasing in air part and monotonous decreasing in dielectric part of the cavity. Their graphical representation forms so-called resonant map that can be used for calculation and identification of resonant frequencies. As an illustration, resonant map of TM_{01p} mode family is shown in Fig.2 together with resonant frequencies calculated by TRM for circular metallic cavity with following dimensions: a=7 cm, h=14.24 cm and $\underline{\varepsilon}_r = 80$ (lossless dielectric–dotted lines) or $\underline{\varepsilon}_r = 80 - j7.2$ (low lossy dielectric–solid lines).

It can be noticed that resonant frequency curves calculated by TRM start from points corresponding to the resonant frequencies of empty cavity:

$$f_{ea}^2(0) = (\ell f_0)^2 + f_{c0}^2 \tag{7}$$

and pass through the characteristic points $rr(\ell k)$ and $aa(\ell k)$. Points rr and aa are the crossing points of the auxiliary resonant and anti-resonant curves, respectively, in air and dielectric part of the cavity. In the direction of filling factor increase, the resonant frequency curve parts are concave between points $aa(\ell k)$ and $rr(\ell k)$ and convex between points $rr(\ell k)$ and $aa(\ell k)$, while for higher values of filling factor after the last $rr(\ell k)$ point, resonant curves follow the auxiliary anti-resonant curve for dielectric part of the cavity given by Eq.(6).

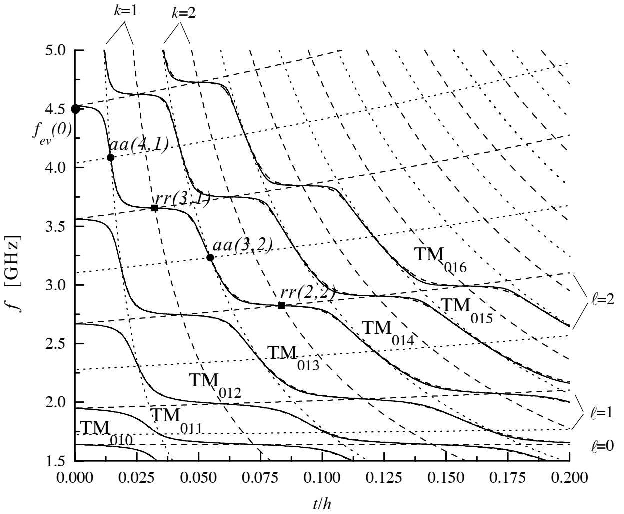

Fig.2 *The resonant map and frequencies for* TM_{01p} *mode family calculated by TRM*

The resonant frequency curves versus filling factor change their shape in the crossing point which means that the second derivation of wanted approximate function should be equal to zero in these points. Introducing two additional points between rr and aa or between aa and rr, a cubic spline approximation can be applied for convex (Fig.3*a*) and concave (Fig.3*b*) resonant curve behaviour modelling. Using two addition points with coordinates (x_1, y_1) and (x_2, y_2), the resonant frequency curve parts are divided into three segments: $[x_0, x_1]$, $[x_1, x_2]$ and $[x_2, x_3]$. For each segment the following cubic spline approximation is used:

$$S3(x) = \frac{M_i}{6h_i}(x - x_{i-1})^3 + \frac{M_{i-1}}{6h_i}(x_i - x)^3 + \left(y_i - \frac{h_i^2 M_i}{6}\right)\frac{x - x_{i-1}}{h_i} + \left(y_{i-1} - \frac{h_i^2 M_{i-1}}{6}\right)\frac{x_i - x}{h_i} \tag{8}$$

where: $x \in [x_{i-1}, x_i]$ for i=1,2,3 and $h_i = x_i - x_{i-1}$. Variables M_i for i=1,2,3 are second derivations of wanted approximate function in points with coordinates (x_i, y_i). M_0=0 and M_3=0, while M_1 and M_2 can be found from the following system of two equations:

$$\frac{x_2 - x_1}{x_2 - x_0} M_2 + 2M_1 = \frac{6}{x_2 - x_0}\left(\frac{y_2 - y_1}{x_2 - x_1} - \frac{y_1 - y_0}{x_1 - x_0}\right) \tag{9}$$

$$\frac{x_2 - x_1}{x_3 - x_1} M_1 + 2M_2 = \frac{6}{x_3 - x_1}\left(\frac{y_3 - y_2}{x_3 - x_2} - \frac{y_2 - y_1}{x_2 - x_1}\right) \tag{10}$$

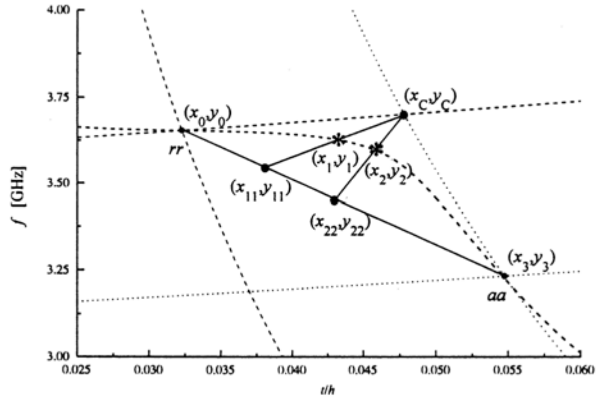

a)

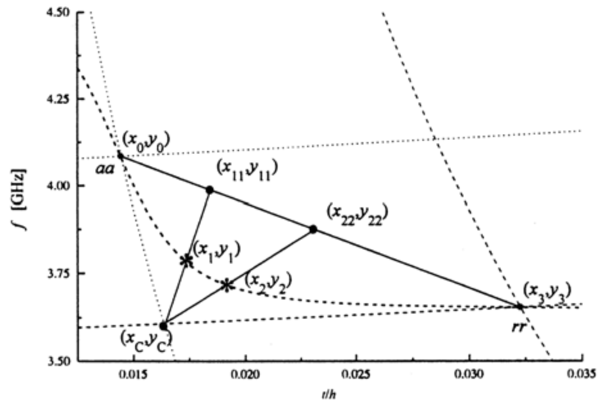

b)

Fig.3 *Additional points choice for best approximation*

How the quality of approximation strongly depends on accurate determination of two additional points coordinates, especially for the case of lossy dielectric slab, they are found empirically for best fitting:

$$u(i)_1 = u(i)_{11} + \left[A * B * 1.1^{\frac{\varepsilon'_r - 40}{20}} + \frac{\varepsilon''_r}{\varepsilon'_r} 0.5^{p/3}\right]\left(u(i)_c - u(i)_{11}\right) \tag{11}$$

$$u(i)_2 = u(i)_{22} + \left[A * B * 1.1^{\frac{\varepsilon'_r - 40}{20}} + \frac{\varepsilon''_r}{\varepsilon'_r} 0.5^{p/3}\right]\left(u(i)_c - u(i)_{22}\right) \tag{12}$$

where $u(1)$ corresponds to x and $u(2)$ corresponds to y coordinate of additional points and

$$u(i)_{11} = u(i)_0 + 0.3\left(u(i)_3 - u(i)_0\right) \text{ for } i\text{=1,2} \tag{13}$$

$$u(i)_{22} = u(i)_0 + 0.7\left(u(i)_3 - u(i)_0\right) \text{ for } i\text{=1,2} \tag{14}$$

Variables x_c and y_c represent the xy coordinates of crossing points for corresponding auxiliary resonant curve in air and anti-resonant curve in dielectric part of the cavity. Parameter

A is 0.45 for concave and 0.5 for convex shape, while parameter B is:

$$B = \begin{cases} 1 & \text{for } \varepsilon'_r \geq 20 \\ 1.2^{\frac{\varepsilon'_r - 20}{\varepsilon'_r}} & \text{for } \varepsilon'_r \leq 20 \end{cases} \tag{15}$$

Intensive investigation has been shown that approximate procedure, presented here, can be applied to low lossy dielectric slabs ($\varepsilon''_r / \varepsilon'_r \leq 0.12$) as well, i.e. resonant frequency curves are still passing through the characteristic points *rr* and *aa* for dielectric materials with small losses.

B. Neural networks

In order to avoid complex and time-consuming mathematical calculations associated with TRM**,** an application of neural networks on resonant frequency determination in cylindrical metallic cavities is suggested in references [15-18]. The first step in cavity modeling was based on use of MLP neural networks while the training data was provided by TRM [15] (Fig.4).

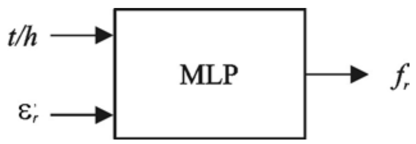

Fig.4 *MLP approach*

As previously mentioned, the main disadvantage of this method was a large number of training data required for the training processes. Size of the training set can be significantly reduced using a hybrid empirical-neural (HEN) model [16,18], on the basic of non-uniform distribution of training samples obtained from approximate procedure and the deviations between results obtained using TRM and approximation approach (Fig.5).

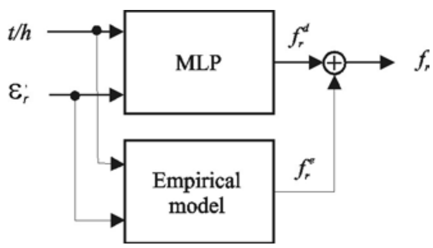

Fig.5 *A hybrid empirical neural mode of cavity*

A special attention is this section will be addressed to the application of the knowledge based neural (KBN) network structure [17,18]. Since, there are explicate expressions for the resonant and anti resonant curves dependence on ε'_r and *t/h*, defined in approximate approach and shown in Fig.2, the basic idea for KBBN approach is implementation of these expressions as activation functions of some neurons in the neural network. The proposed KBNN architecture, with two input parameters and resonant frequency as output parameter, is presented in Fig.6.

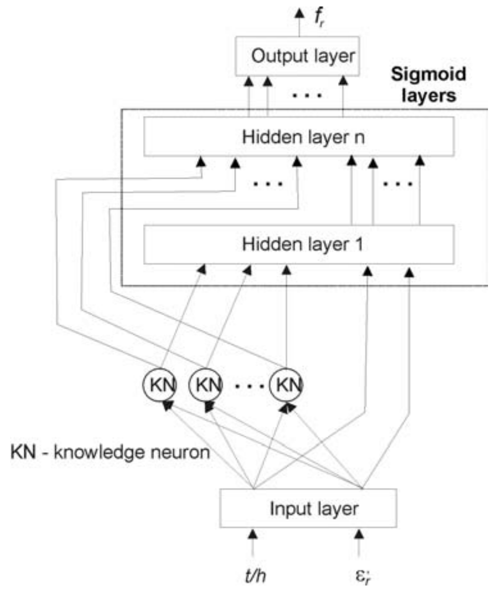

Fig.6 *Knowledge based neural network*

KBNN structure is a modified MLP structure. Namely, a network is consists of neurons grouped into the layers. Beside hidden layers of sigmoid neurons, there are so-called knowledge neurons (KN). Activation functions, as modified expressions of the resonant and anti-resonant curves in air $\left(f_a^i\right)$ and dielectric part $\left(f_d^j\right)$ of the cavity, are realized through the layer of knowledge neurons. First type of KN uses the activation function

$$f_a^i = \sqrt{\frac{a(i)}{\left(1 - \frac{t}{h}\right)^2} + b(i)} \tag{16}$$

whereas the second type uses the activation function

$$f_d^j = \sqrt{\frac{a(j)}{\varepsilon'_r} + \frac{b(j)}{\varepsilon'_r \cdot \left(\frac{t}{h}\right)^2}} \tag{17}$$

where: $a(i)$ and $b(j)$ represent trainable parameters, i=1,2,...I and j=1,2,…J. It has been found that the symmetrical case in which the number of both types knowledge neurons is equal (I=J) gives the best results. As a result, KBNN models the following dependence

$$f_r = F\begin{pmatrix} f_a^{(1)}, \ldots, f_a^{(2)}, \ldots f_a^{(V)}, \\ f_d^{(1)}, \ldots, f_d^{(d)}, \ldots, f_d^{(D)}, t/h, \varepsilon'_r \end{pmatrix} \tag{18}$$

Application of such structure leads to a increasing of network generalization capabilities yielding to a further reducing of required number of training samples. Furthermore, this approach eliminates need for the use of empirical model used in HEN approach making resonant frequency determination faster.

C. TLM Method

In the conventional TLM time-domain method, electromagnetic field strength in three dimensions, for a specified mode of oscillation in a cylindrical metallic cavity, is modelled by filling the field space with a network of link lines and exciting a particular field component through incident voltage pulses on appropriate lines [20]. Electromagnetic properties of different mediums in the cavity are modelled by using a 3-D network of interconnected nodes (Fig.7*a*), a typical structure being the symmetrical condensed node (SCN) [30]. Each node describes a portion of the medium shaped like a cuboid (Cartesian rectangular mesh) or a slice of cake (Non-Cartesian cylindrical mesh) depending on the geometry of modelled cavity (Fig.7*b*).

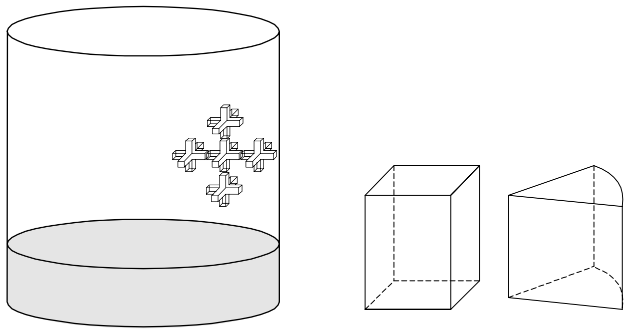

a) *b*)

Fig.7
a) *A cavity space modelled by the mesh of TLM nodes*
b) *A portion of a medium in rectangular or cylindrical grid*

Additional stubs can be incorporated into TLM model to account for inhomogeneous materials and/or electric and magnetic losses in the modelled mediums. For the case of homogeneous lossy dielectric, given the effective electrical conductivity σ_e, lossy 'electrical' element for the 3-D TLM is defined as [30]:

$$G_e = \sigma_e \, f(\Delta x, \Delta y, \Delta z) \tag{19}$$

where Δx, Δy and Δz are dimensions of TLM node in the *x*, *y* and *z* directions respectively.

Complex permittivity is connected to effective electrical conductivity in the form of:

$$\underline{\varepsilon} = \varepsilon_0 \underline{\varepsilon}_r = \varepsilon_0 \varepsilon_r' - j\sigma_e / \omega \tag{20}$$

which gives loss tangent at particular frequency *f* as:

$$\tan\delta = \frac{\sigma_e}{2\pi f \varepsilon_0 \varepsilon_r'} \tag{21}$$

For lossy inhomogeneous dielectric sample, as in the case of tunnel type microwave applicators, TLM approach is based on using a non-uniform mesh with high resolution. Dielectric is divided into a sufficient number of regions with equal length in the direction of inhomogeneity [26] (Fig.8). Each of these regions is then considered as a lossy homogenous dielectric which can be modelled using Eqs.(19-21). Resolution of the applied TLM mesh for each region of dielectric sample (number of nodes n_i) varies in the direction of inhomogeneity and it depends on its constant relative permittivity. TLM mesh resolution is also different in dielectric and air layer ($\Delta z_1^d / \Delta z_2^a < 1$) as a result of the propagation velocity in the dielectric sample square root of permittivity lower than in free space.

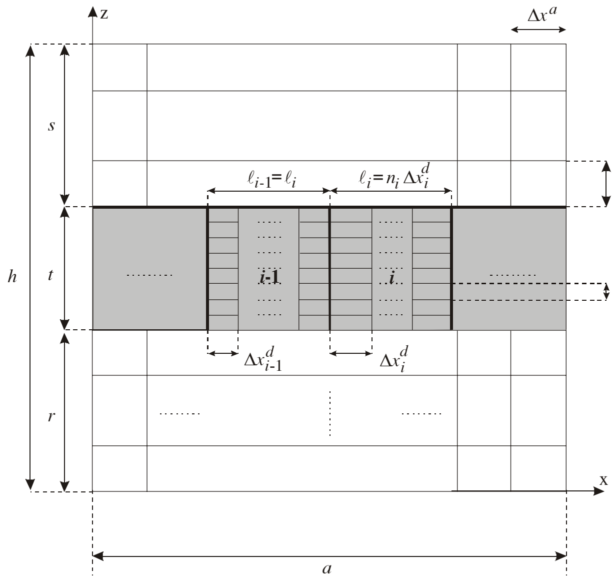

Fig.8 *A non-uniform TLM mesh for inhomogeneous dielectric modelling*

Another type of inhomogeneity, as a result of load shape is investigated in [27]. Having in mind that in many practical cases of microwave heating cavities application, dielectric material in the cavity can have more complex shape, several characteristic geometries of the dielectric load are modelled using 3-D TLM algorithm for orthogonal curvilinear mesh. Here, the most complicated shape where dielectric sample is sloped at some angle in regard to cavity base is given.

A sloped lossy dielectric sample (total cavity load inhomogeneous in *r*, θ and z directions) (Fig.9) is modelled in the form of the *n* dielectric layers (Fig.10*a*) of small thickness *dz* (Fig.10*b*). The cavity space is divided into non-uniform grids in all three directions. The plane interface B-B*'*, formed by two regions ((1) and (2)) with different relative permittivity $\varepsilon_0 \underline{\varepsilon}_r$ and ε_0, respectively, is defined by vector of points which location in radial direction r_{b_s} is determined by the resolution of the mesh in θ direction and it can be written for *k*-th dielectric layer:

$$r_{b_s} = \frac{x_k}{\cos((2s-1)\, d\theta / 2)} \quad \text{for} \quad s = 1, \ldots q \tag{22}$$

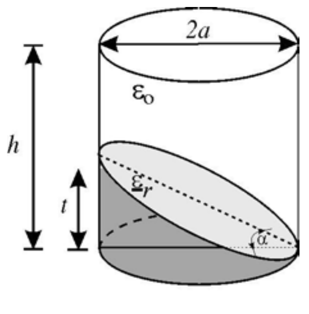

Fig.9 *A circular metallic cavity loaded with lossy dielectric sample sloped at angle α in regard to cavity base*

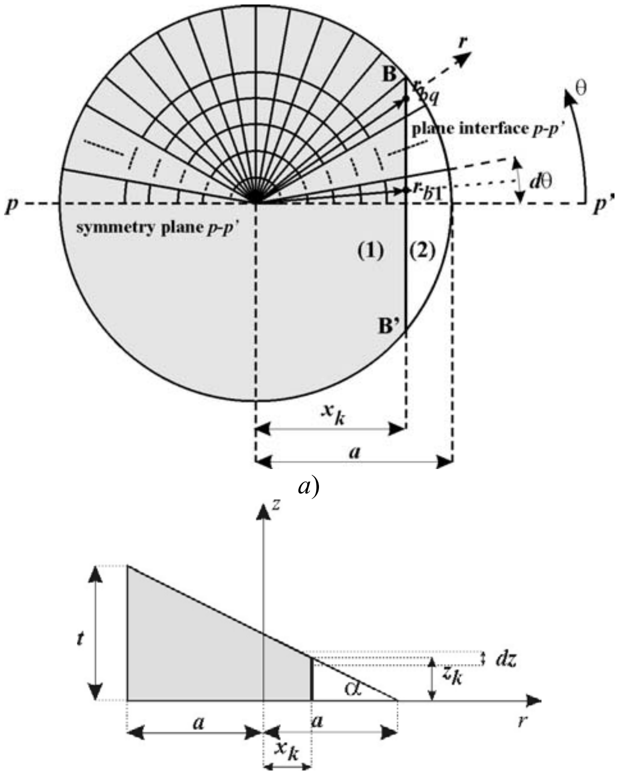

Fig.10 *The k-th layer (k=1,..., n) of the lossy dielectric sample sloped in regard to cavity base in:*
a) the rθ plane, b) the rz plane

Distance between plane interface for k-th layer and cavity centre, x_k, can be found from Fig.10*b*:

$$\frac{z_k}{a - x_k} = tg\alpha \tag{23}$$

where is: α - slope angle of the dielectric sample in regard to base of the cavity, a – radius of the cavity and z_k – distance between centre of k-th dielectric layer and base of the cavity. In the modelling approach, it is used that for $r_{i,j} \le r_{b_s}$ the cell belongs to region (1) and for $r_{i,j} > r_{b_s}$ the cell belongs to region (2). In the regions with higher cell radius $r_{i,j}$, finer TLM cylindrical mesh is applied in order to keep an error, made by using this rule, small.

In previous TLM models, an impulse excitation is used to establish a desired mode distribution in the modelled cavity. However, this way of enhancing the wanted TE or TM mode is clearly different from the experimental procedure conducting in [11] where a small probe, placed inside the cavity, is used as an excitation (Fig.11). This difference in TLM and experimental model regarding the cavity excitation may cause that the TLM results of resonant frequencies and field strength are shifted from the experimental ones.

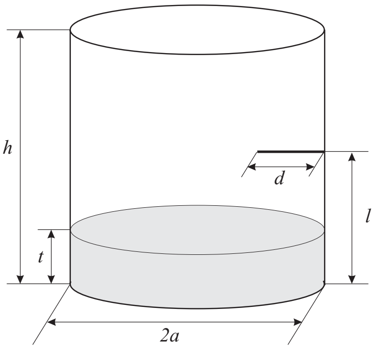

Fig.11 *A loaded cylindrical cavity with a real feed probe*

Also, in practice, depending on the position and the form of excitation (probe, loop, waveguide or slots), the number of modes excited in the cavity will be different from the theoretical case. For instance, placing the coaxial cable in the middle of cavity height will not generate modes with even-mode numbers in z-plane. From the remaining odd-mode numbers some modes will not be excited, depending on whether they have an electric field component in the direction of the source electric field. The resulting electric field strength will then be given by the sum of the modes excited in the cavity. Another problem is accurate identification of modes. Although the reflection characteristic (S_{11}) plots give the number of modes in the cavity, they do not indicate exactly which modes are present. The probe presence also tends to shift the modes and sometimes split degenerate modes.

Recent improvement in the form of TLM wire node [30] can be used to efficiently account for probe presence inside the cavity and allows for more accurate numerical investigation of the real excitation influence to the resonant frequencies. Wire node is based on SCN with one small modification of additional link and stub lines interposed over the exiting network to account for increase of capacitance and inductance of the medium caused by wire presence. Wire network is usually placed into the centre of the TLM nodes to allow complex wire structures modelling, e.g. wire junctions and bends. The single column of TLM nodes, through which wire conductor passes, can be used to approximately form the fictitious cylinder which represents capacitance and inductance of wire per unit length. Its effective diameter, different for capacitance and inductance, can be expressed as a product of factors empirically obtained by using known characteristics of TLM network and the mean dimensions of the node cross-section in the direction of wire running.

Requirement that the equivalent radius of fictitious cylinder is constant along nodes column can be easily met in a rectangular grid. However, in the cylindrical grid for wire conductor in the radial direction, mean cross-section dimensions of TLM nodes, through which wire passes, are changeable making difficult to preserve distributed capacitance and inductance of wire per unit length. Because of that, a rectangular grid is more suitable for modelling of cylindrical cavity with circular cross-section. At the same time, the numerical errors introduced by describing boundary surfaces of the modelling cavity in a step-wise fashion are reduced applying the TLM mesh higher resolution around cavity walls.

III. NUMERICAL ANALYSIS

The approximate procedure presented in section II.A will be illustrated on the example of cylindrical metallic cavity with circular cross-section (Fig. 1, a=7 cm and h=14.24 cm) [14]. The load is lossy homogeneous slab placed at the bottom of the cavity and whose complex relative permittivity is $\underline{\varepsilon}_r = 80 - j9.6$. The resonant frequency curves of TM_{01p} mode family obtained using the approximate procedure (short dotted lines) are shown in Fig.12 as well as the solutions of complex transcendent characteristic equation defined from TRM (solid lines). An excellent agreement between the results of these two approaches can be observed.

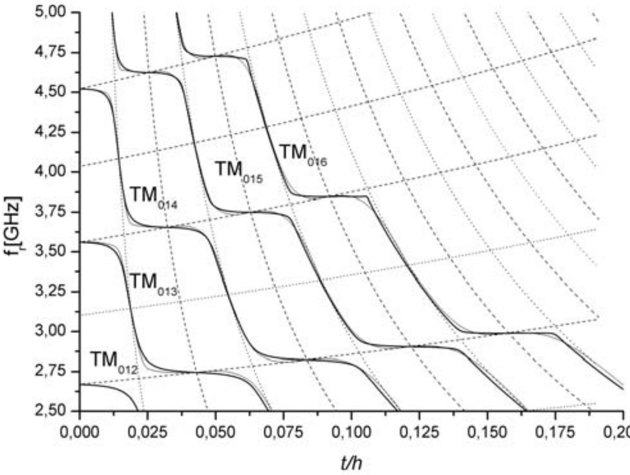

Fig.12 *The resonant frequencies of* TM_{01p} *mode family obtained using: a) approximate procedure (short dotted lines), b) MTR (solid lines)*

The circular metallic cavity with the same dimensions as in previous example will be used to show an advantage of KBN network in comparison with classical MLP network [17]. Two models are selected for simulation: MLP4-12-12 model (12 neurons in each of two hidden layers) and KBNN3-4-16-16-16 model (16 neurons in each of three hidden layers and 4 knowledge neurons-2 for each activation function). The number of training data samples is 80. Simulation results for TM_{112} mode, calculated using these two models as well as referent curve obtained using TRM are shown in Fig.13. As expected, the KBNN3-4-16-16-16 model results have better agreement with referent values than results of corresponding MLP model. The developed models are also used for 3-D presentation of resonant frequency dependence in function of dielectric relative permittivity and filling factor (Fig.14*a* for MLP4-12-12 and Fig.14*b* for KBNN3-4-16-16-16). The used training data set is too small for MLP network training which explains the lower accuracy achieved with this model.

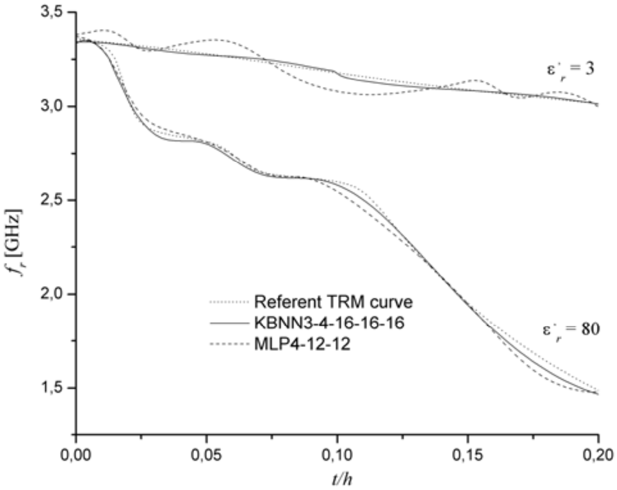

Fig.13 *Simulation results comparison of the MLP4-12-12 and KBNN3-4-16-16-16 model with referent results*

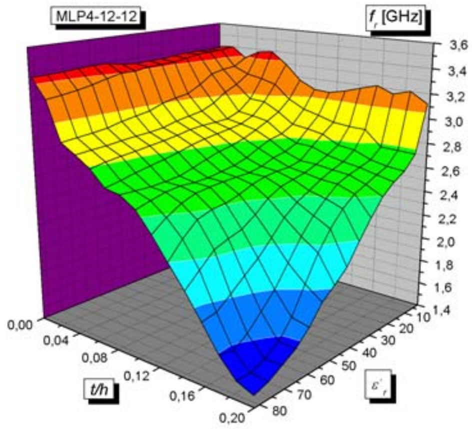

a)

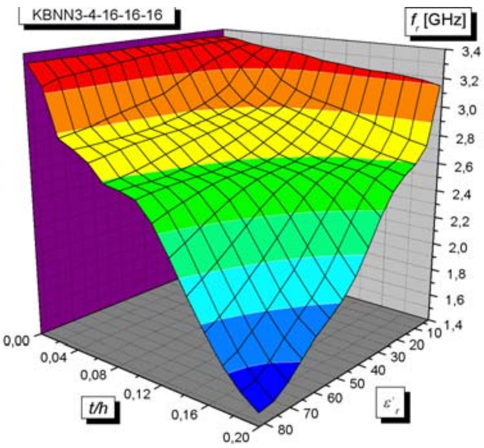

b)

Fig.14 *Three-dimensional presentation of* TM_{112} *mode obtained using: a) M4-12-12 model, b) KBNN3-4-16-16-16 model*

Tunnel type microwave applicator is the first of several examples, considered in this paper, where an advantage of TLM method in comparison with other presented approaches, is clearly indicated. Movable applicator load (dielectric material on a conveyor belt), which mostly contains water as a dominant element within itself, could be represented in the form of dielectric slab raised from the bottom of the rectangular metallic cavity [26] (Fig.15, a=35 cm, b=37 cm, h=26.9 cm). Its electrical parameters are continually changed along the moving direction depending on the temperature variation in the particular load sample. As a result, the applicator load is a lossy inhomogeneous dielectric slab. TRM with a modification in the form of integral characteristic equation [7] faces up to the great difficulties of numerical nature and can give a satisfactory solution only for lossless load placed at the bottom (r=0) or in the middle of the cavity (r=s).

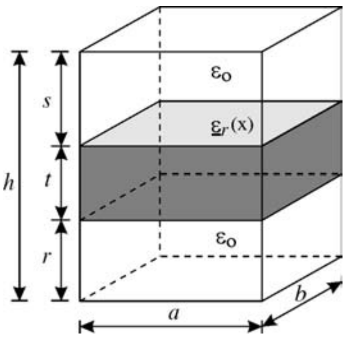

Fig.15 *A loaded rectangular metallic cavity*

Numerical results of resonant frequencies for TE_{101} mode versus filling factor t/h, calculated using integral TRM are shown in Fig.16 for lossless inhomogeneous dielectric slab placed at the bottom of the cavity (r=0) with linear temperature variation (5-50) ^{o}C (dashed line) and for two hypothetical cases of homogeneous lossless sample with extreme temperature: T=5 ^{o}C and T=50 ^{o}C (dotted lines). In the same figure, the star symbols indicate the results obtained using the TLM model (Fig.8) with impulse field excitation H_z to enhance the TE_{10p} modes inside the cavity. There is an excellent agreement between TLM and integral TRM results.

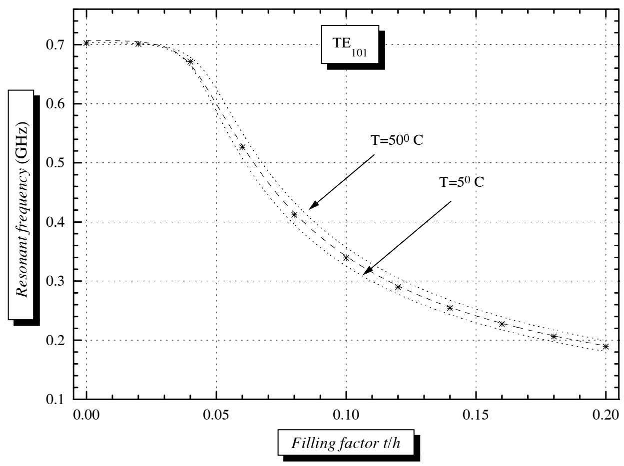

Fig.16 *The resonant frequency versus filling factor t/h and for lossless sample placed at* $r = 0$*, calculated using: 3-D TLM method (*) and integral TRM (dashed line)*

The resonant frequency curve of TE_{101} mode versus filling factor t/h, obtained using suggested TLM model, for the real practical case when inhomogeneous lossy dielectric sample is located at the height r=4 cm from the bottom of the cavity is shown in Fig.17. As it can be seen from Figs.16 and 17, the resonant frequencies are within the limits determined by two hypothetical homogenous dielectric samples. Further investigation of influence of inhomogeneous load location, thickness and losses on applicator mode tuning behaviour can be found in [26].

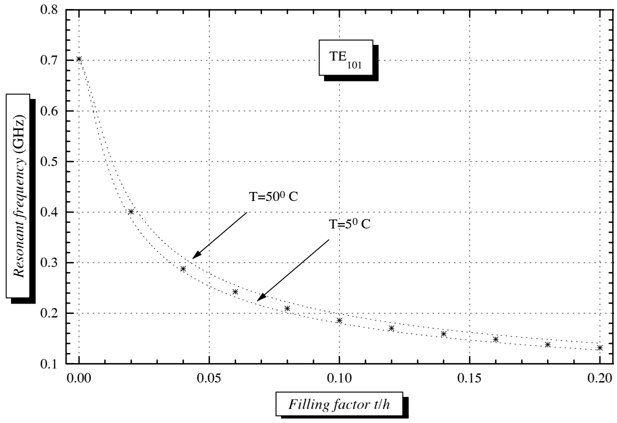

Fig.17 *The resonant frequency versus filling factor t/h and for lossy sample raised at* $r = 4$ *cm , calculated using: 3-D TLM method*

The next example is TLM modelling of dielectric sample with complex geometry. For that purpose, a circular metallic cavity with dimensions a=7 cm and h=14.24 cm (Fig.9) is investigated [27]. The load shape in Fig.9 is realised in the experimental set-up using the cavity loaded by water and sloped at angle α in regard to its base, while a model shown in Fig.10 is used for TLM modelling. Complex relative permittivity of water is calculated from Debye's formula at a temperature T=20°. The TLM cylindrical mesh is excited with impulse excitation H_θ to enhance the TM_{01p} mode. The circle in the centre of the mesh is considered as an open-circuit boundary. The same mode is established in the experimental cavity using coupling loop at the end of the coaxial line. The number of nodes in the z direction has been increased for higher values of α keeping the accuracy of modelling. Symmetry is used around a plane running through the axis of the cavity (symmetry plane p-p'). Resonant frequencies calculated using TLM model as well as measured results are given in Table.1 for several values of α.

α=5°		α=15°		α=25°		α=35°		α=45°	
f(GHz) (TLM)	f(GHz) (Exp.)	f(GHz) (TLM)	f(GHz) (Exp.)	f(GHz) (TLM)	f(GHz) (Exp.)	f(GHz) (TLM)	f(GHz) (Exp.)	f(GHz) (TLM)	f(GHz) (Exp.)
1.581	1.60	1.589	1.62	1.626	1.62	1.604	1.61	1.613	1.63
1.702	1.72	1.772	1.79	1.834	1.87	2.043	1.98	2.046	2.08
2.358	2.37	2.417	2.42	2.457	2.47	2.526	2.59	2.849	2.86
2.776	3.05	2.805	3.07	2.859	3.09	2.888	3.12	3.453	3.53

Table 1 *Numerical and experimental results of the resonant frequencies for several values of α*

Some deviations, noted especially at higher frequencies, can be explained mostly both by the stair-casing description of the dielectric incline and the difference between TLM and experimental model regarding the cavity excitation, i.e. wire presence in the experimental cavity. The complete analysis for different load shapes and their influence on the resonant frequencies in cylindrical metallic cavity are given in [27].

The last example will illustrate the influence of real feed probe length to the resonant frequencies of circular metallic cavity loaded with lossy homogeneous dielectric sample [28] (Fig.11, a=7 cm, h=14.24 cm, t=3 cm). How in experimental set-up water is used as a cavity load, complex relative permittivity of dielectric sample is calculated from Debye's formula. A feed probe with radius r=0.5 mm, is placed at the height l=7.4 cm from the bottom of the cavity, slightly different from h/2, in the r direction. In this way, it is possible to excite modes having r-component of the electrical field in the cavity. Feed probe, modelled through TLM wire node, is fed by real voltage source V_{source}=1 V and R_{source}=50 Ω. The resonant frequencies are determined from the reflection characteristic (S_{11}) plot.

The obtained TLM numerical results and the experimental results of resonant frequencies for modes in the frequency range f=[1.5-3.0] GHz, versus probe length are shown in Fig.18. The circle symbols indicate the results obtained using TLM method with wire node to account for probe presence (real probe TLM) and triangle ones indicate the experimental results. The straight lines present the values of resonant frequencies calculated using the conventional TLM method with an impulse excitation (impulse TLM). Also, a quarter-wavelength curve is presented in order to identify the areas of capacitive and inductive character of probe input impedance. As it can be seen, resonant frequency dependence of feed probe length is significant and different for these two areas. Also, as expected, TLM results obtained with wire node follow the experimental ones much better than the conventional results. Reflection characteristic plot (S_{11}) for the probe length d=5 cm is shown in Fig.19. More about the influence of probe presence and its dimension on cavity mode tuning behaviour can be found in [28].

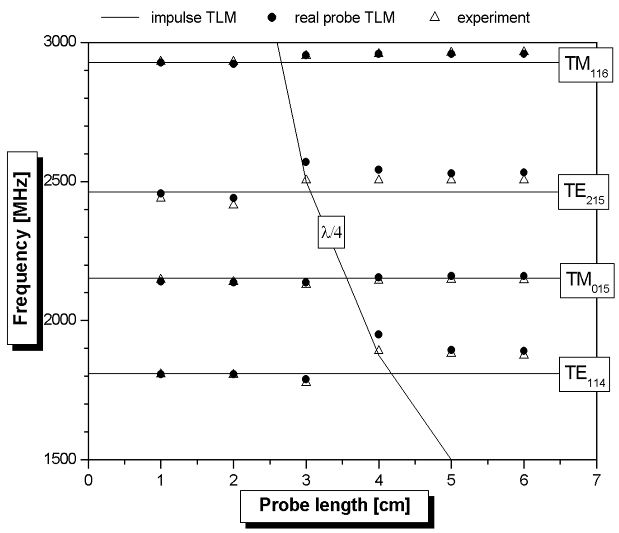

Fig.18 *Resonant frequencies versus probe length*

IV. Conclusion

In this paper, a short review of techniques used for modelling and analysis purposes of cylindrical metallic cavities together with the numerical results mostly experimentally verified are given. The presented techniques can be very useful from practical point of view in the microwave heating applicators designing. Future researches will be divided into two parts: use of TLM z-transform method for accurate modelling of frequency dependant dielectric materials and the development of hybrid TLM-neural networks models.

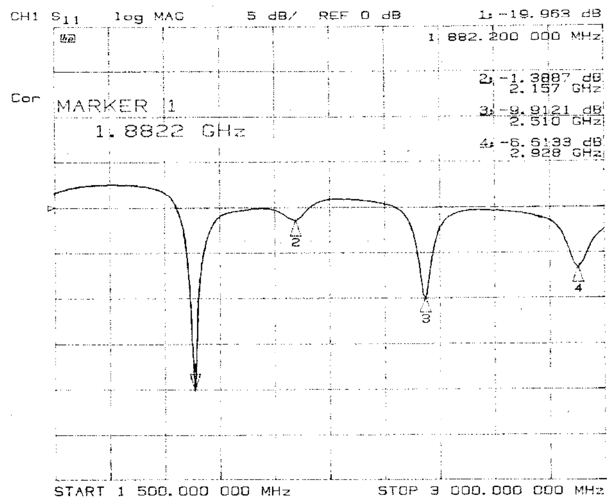

a)

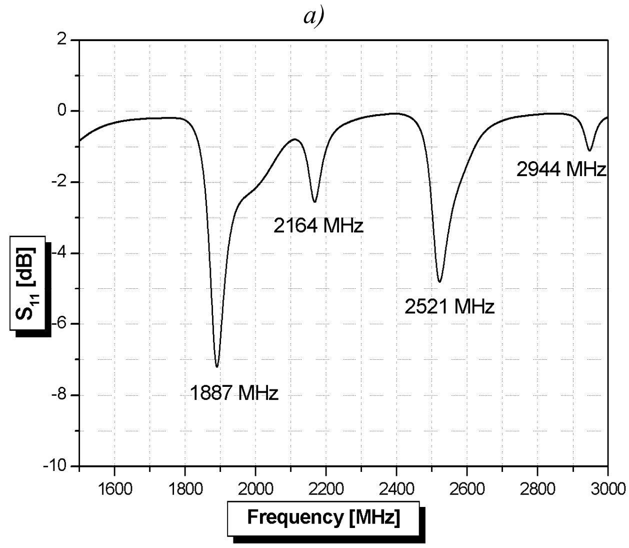

b)

Fig.19 S_{11} *plot in the frequency range f=[1.5-3.0] GHz for the probe length d=5 cm, obtained: a) experimentally, b) using TLM method*

References

[1] T.V.Chow Ting Chan, H.C.Reader, *Understanding Microwave Heating Cavities,* Artech House, Inc, 2000.

[2] T.G.Mihran, *Microwave Oven Mode Tuning by Slab Dielectric Loads*, IEEE Transactions on Microwave Theory and Techniques, Vol.26, No.6, pp.381-387, 1978.

[3] Shen Zhi-Yuan, *An Analysis of the Loading Effects of the Box-type Microwave Applicator*, Journal of Microwave Power, Vol.15, No.3, pp.155-167, 1980.

[4] E.El-Sayed, *Influence of Loaded Location in Mode Tuning of Microwave Ovens*, Journal of Microwave Power and Electromagnetic Energy, Vol.18, No.2, pp.197-207, 1985.

[5] M.Mladenovic, A.Marincic, B.Milovanovic, *Mode Tuning of Microwave Resonator Loaded with Lossy Multilayer Dielectric,* Journal of Microwave Power and Electromagnetic Energy, Vol.24, No.3, pp.166-177, 1989.

[6] M.Mladenovic, *Numerical and Experimental Analysis of Loaded Resonator in Dynamic Mode at High Level Power,* Ph.D. Thesis, Faculty of Electronic Engineering, University of Nis, Yugoslavia, 1991.

[7] M.Mladenovic, A.Marincic, B.Milovanovic, *Calculation of Resonances of Microwave Resonator Loaded with Inhomogeneous Dielectric Layer*, Electronics Letters, Vol.27, No.24, pp.2215-2216, 1991.

[8] M.Mladenovic, A.Marincic, B.Milovanovic, S.Ivkovic, *Identification of Resonant Modes in a Loaded Microwave Rectangular Cavity*, Journal of Microwave Power and Electromagnetic Energy, Vol.31, No.1, pp.30-34, 1996.

[9] A.Baysar, J.L.Kuester and S.El-Ghazaly, *Theoretical and Experimental Investigations of Resonance Frequencies in a Microwave Heated Fluidized Bed Reactor,* IEEE MTT-S Digest, pp.1573-1576, 1992.

[10] B.Milovanovic, S.Ivkovic, N.Doncov, D.Djordjevic, *Resonant Frequencies Determination of Circular Cylindrical Cavities Loaded By One Lossy Dielectric Slab*, Yugoslav IEEE MTT Chapter Informer, No.4, pp.33-37, 1996.

[11] S.Ivkovic, B.Milovanovic, A.Marincic and N.Doncov, *Theoretical and Experimental Investigations of Resonance Frequencies in Loaded Cylindrical Microwave Cavity,* Proc. of the 3rd IEEE TELSIKS'97 Conference, Nis, Yugoslavia, pp.306-309, 1997.

[12] B.Milovanovic, S.Ivkovic, N.Doncov, D.Djordjevic, *Mode Tuning of Multilayer Cylindrical Cavities with Circular and Elliptical Cross-section*, Journal of Microwave Power and Electromagnetic Energy, Vol.33, No.1, pp.49-56, 1998.

[13] C.Balanis, *Advanced Engineering Electromagnetics*, John Wiley & Sons, Inc, USA, 1989.

[14] B.Milovanovic, S.Ivkovic, A.Atanaskovic, *An Approximate Procedure for Resonant Frequency Determination of the Loaded Cylindrical* Cavity, Journal of Microwave Power and Electromagnetic Energy, Vol.34, No.3, pp.185-191, 1999.

[15] B.Milovanovic, Z.Stankovic, S.Ivkovic, *Modelling of the Cylindrical Metallic Cavity Loaded by Lossy Dielectric Slab Using Neural Networks*", Proc. of the 5th Conference on Neural Network Application in Electrical Engineering - NEUREL 2000, Belgrade, Yugoslavia, pp.141-145, 2000.

[16] B.Milovanovic, Z.Stankovic, S.Ivkovic, *Modelling of the Cylindrical Metallic Cavity with Circular Cross-section using Neural Networks,* Proc. of the 10th Mediterranean Electrotechnical Conference – MELECON 2000, Vol.2, pp.449-452, 2000.

[17] Z.Stankovic, B.Milovanovic, S.Ivkovic, *Microwave Cylindrical Cavity Applicators Modelling using Knowledge Based Neural Network*, Proc. of the 5th IEEE TELSIKS'01 Conference, Nis, Yugoslavia, pp.687-690, 2001.

[18] B.Milovanovic, V.Markovic, Z.Marinkovic, Z.Stankovic, *Some Applications of Neural Networks in Microwave Modelling*, Journal of Automatic Control, University of Belgrade, Yugoslavia, Vol.13(1), pp.39-46, 2003.

[19] K.S.Kunz, R.J.Luebbers, *The Finite Difference Time Domain for Electromagnetics*, CRC Press, 1993.

[20] C.Christopoulos, *The Transmission-Line Modelling Method*, IEE/OUP Press, 1995.

[21] F.Liu, I.Turner, M.E.Bialkowski, *A Finite-Difference Time-Domain Simulation of Power Density Distribution in a Dielectric Loaded Microwave Cavity*, Journal of Microwave Power and Electromagnetic Energy, Vol.29, No.3, pp.138-148, 1994.

[22] L.Ma, D.L.Paul, N.Pothecary, C.Railton, J.Bows, L.Barrat, J.Mullin, D.Simons, *Experimental Validation of a Combined Electromagnetics and Thermal FDTD Model of a Microwave Heating Process*, IEEE Transactions on Microwave Theory and Techniques, Vol.43, No.11, pp.2565-2572, 1995.

[23] M.F.Iskander, R.L.Smith, A.O.M.Andrade, H.Kimrey, L.M.Walsh, *FDTD Simulation of Microwave Sintering of Ceramics in Multimode Cavities*, IEEE Transactions on Microwave Theory and Techniques, Vol.42, No.5, pp.793-799, 1994.

[24] D.H.Choi, W.J.R.Hoefer, *The Finite-Difference-Time-Domain Method and its Application to Eigenvalue Problems*, IEEE Transactions on Microwave Theory and Techniques, Vol.34, No.12, pp.1464-1470, 1986.

[25] R.A.Desai et all, *Computer Modelling of Microwave Cooking using the Transmission-line Model*, IEE Proceedings, Pt.A, Vol.139, No.1, pp.30-37, 1992.

[26] B.Milovanovic, N.Doncov, A.Atanaskovic, *Tunnel Type Microwave Applicator Modelling using TLM Method*, Problems in Modern Applied Mathematics: A Series of Reference Books and Textbooks: Mathematics and Computers in Science and Engineering, WSES Press, pp.327-332, 2000.

[27] B.Milovanovic, N.Doncov, *TLM Modelling of the Circular Cylindrical Cavity Loaded by Lossy Dielectric Sample of Various Geometric Shapes*, Journal of Microwave Power and Electromagnetic Energy, Vol.37, No.4, pp.237-247, 2002.

[28] B.Milovanovic, A.Marincic, N.Doncov, V.Markovic, J.Jokovic, A.Atanaskovic, *Analysis of Real Feed Probe Influence to the Resonant Frequencies and Field Distribution in the Cylindrical Metallic Cavity using 3D TLM Method*, Microwave Review, A Publication of Yugoslav Society for Microwave Theory and Techniques and Yugoslav IEEE MTT-S chapter, No.1, Vol.9, pp.50-55, 2003.

[29] V.Trenkic, A.J.Wlodarczyk, R.Scaramuzza, *Modelling of Coupling Beetween Transient Electromagnetic Field and Complex Wire Structures*, International Journal of Numerical Modelling: Electronic Networks, Devices and Fields, Vol.12, No.4, pp.257-273, 1999.

[30] V.Trenkic, *The Development and Characterization of Advanced Nodes for TLM Method*, Ph.D. Thesis, University of Nottingham, UK, 1995.